Available online at www.sciencedirect.com
ScienceDirect
Agricultural and Forest Meteorology 142 (2007) 156–169
AGRICULTURAL AND FOREST METEOROLOGY
www.elsevier.com/locate/agrformet

Impact of agriculture, forest and cloud feedback on the surface energy budget in BOREAS

Alan K. Betts [a,*], Raymond L. Desjardins [b], Devon Worth [b]

[a] *Atmospheric Research, 58 Hendee Lane, Pittsford, VT 05763, United States*
[b] *Agriculture and Agri-Food Canada, 960 Carling Avenue, Ottawa, Ont. K1A 0C6, Canada*

Received 7 January 2005; received in revised form 15 May 2006; accepted 22 May 2006

Abstract

We explore the impact of agriculture, forest and cloud feedback on the surface energy budget using data obtained using a research aircraft, mesonet towers and model data. The forest has an order of magnitude larger roughness length, a lower albedo, a much smaller seasonal cycle in surface Bowen ratio (BR) and a weak mid-summer maximum of CO_2 uptake compared to agricultural areas, which have much smaller BR and much higher mid-summer CO_2 uptake, but a net CO_2 release and much reduced evaporation in spring and fall. Higher surface temperatures and the higher albedo over agricultural land reduce R_{net} near local noon in the warm season by about 50 W m^{-2} in comparison with the adjacent boreal forest. The annual averaged R_{net}, derived from 2 years of tower data, is 14 W m^{-2} less over grass sites than over forest sites. A reanalysis time-series for the BOREAS southern study area shows the coupling on daily timescales between the surface energy partition, the mean boundary layer depth, the cloud field and the long-wave and short-wave radiation fields. The albedo of the cloud field, the cloud short-wave forcing at the surface, varies over the range 0.1–0.8 with decreasing surface BR, and plays a major role in the surface energy budget. We estimate that this cloud feedback may increase albedo by 0.13 and reduce R_{net} by 25 W m^{-2} in summer over agricultural land.

Keywords: Surface energy balance; Land-cover change; Agriculture; Boreal forest; Cloud feedback

1. Introduction

Many modeling studies have examined the impact of land use on climate. A large number have addressed the feedback of land-surface properties and the biosphere on climate in the tropics (e.g. Charney et al., 1977; Walker and Rowntree, 1977; Kitoh et al., 1988; Sud et al., 1988; Xue and Shukla, 1993; Xue, 1997). Recent studies (Levis et al., 1999; Brovkin et al., 2003) have addressed the existence of different equilibrium states at high latitudes where temperature limits growth of the boundary layer. There have been fewer studies of the impact of land use for agriculture replacing forests at northern latitudes. Betts (2001) estimated that northern mid-latitude agricultural regions were approximately 1–2 °C cooler in winter and spring in comparison with their previously forested state, due primarily to deforestation increasing the surface albedo during periods of snow cover. Betts (2000) has discussed the relative climatic importance of albedo and CO_2 uptake for grass and forest landscapes at high latitudes. Forests have a lower albedo, especially in winter and early spring, when the snow is shaded from the high zenith angle sun by the canopy. Forests are rougher, but the impact of this on the surface energy budget in mid-continent is unclear. Typically, conifers have the longest

* Corresponding author. Fax: +1 802 483 6167.
E-mail address: akbetts@aol.com (A.K. Betts).

0168-1923/$ – see front matter
doi:10.1016/j.agrformet.2006.08.020

growing season, and crops (other than grass) the shortest, with deciduous species like aspen in between. Trees frequently have deeper rooting depths than crops, but in the boreal landscape, moss layers are also important to the landscape hydrology of wet conifers (Price et al., 1997; Betts et al., 2001a). Crops in mid-summer have a much lower stomatal resistance than conifers, which increases evaporation (and CO_2 uptake) and lowers cloud-base. Generally more evaporation and a lower cloud base means more cloud cover, reduced surface net short-wave, and outgoing longwave radiation, with an overall reduction in net radiation.

Using a mix of observations and model data we address some of these issues. First we compare the surface impact of agriculture and forest using observations made during the Boreal Ecosystem Atmosphere Study (BOREAS: see Sellers et al., 1997). During the 1994 and 1996 summer field campaigns of BOREAS, the Canadian National Research Council (NRC) Twin Otter research aircraft made low altitude measurements of the exchange of energy and trace gases over the boreal forest (MacPherson, 1996; MacPherson and Bastian, 1997). In the southern study area (SSA) in Saskatchewan, measurements were also made over an agricultural area, from the Prince Albert airport to the flux tower study area over the forest near 53.9°N, 105°W. For most days, we have data collected over the agricultural area before and after data collected over the forest, some 50 km to the north. We will compare the surface energy and gas exchanges over the forest and agricultural land (pasture, canola and wheat). There were 22 days with paired data in 1994, evenly divided between the three intensive field campaigns in spring, summer and autumn, and 7 additional days in the 1996 summer campaign. There were also 10 mesonet sites operating during BOREAS: 2 over grass and 7 over predominantly coniferous forest (Shewchuk, 1997). For the years 1994 and 1995, we generated daily means of incident and reflected short-wave and net radiation for each site, and use these to compare the surface energy budget and albedo of forest and grassland sites over the annual cycle. Finally we discuss the feedback between the surface BR and the cloud and radiation fields using model time-series data from the recent European Centre for Medium-range Forecasts (ECMWF) reanalysis.

2. Aircraft data

2.1. Instrumentation

The instrumentation on board the NRC Twin Otter and the measurement of surface energy budgets and trace gas fluxes during the BOREAS campaign have been well described (e.g. MacPherson, 1996; MacPherson and Bastian, 1997; Desjardins et al., 1997; Zhu et al., 1999; Desjardins et al., 2000). The reliability of absolute values, resolution and frequency response of many of these instruments are summarized in Desjardins and MacPherson (1991). The aircraft is instrumented to measure the three orthogonal components of atmospheric motion and the vertical wind velocity is calculated and filtered in real time. Combining fast response measurements of CO_2 concentration, H_2O concentration and air temperature (T_a) using the eddy covariance technique (Desjardins et al., 2000), yields fluxes of CO_2, sensible (H) and latent heat (λE, where E is the evaporative flux and λ is the latent heat of vaporization). Flux data were linearly detrended and corrected for time lags between sensors (MacPherson, 1996), and CO_2 fluxes are corrected for density. Net radiation (R_{net}) was calculated by summing up short- and long-wave components. Incident (SW_{down}) and reflected (SW_{up}) short-wave radiation were measured directly. Outgoing long-wave radiation (LW_{up}) was calculated using the Stephan–Boltzman law and measured surface temperature (T_s), assuming an emissivity of 0.98. Incoming long-wave radiation (LW_{down}) was similarly calculated (MacPherson, 1996) from T_a as

$$LW_{down} = 1.20 \times \sigma \times T_a^4 - 171.0 \quad (1)$$

where σ is the Stephan–Boltzman constant. This technique for calculating R_{net} has agreed well with tower R_{net} measurements in the SSA (Desjardins et al., 1997). A 'Greenness index' for the vegetation below the flight track is also computed as the ratio of measured near-infrared (730 nm) to red (660 nm) radiation.

2.2. Flight patterns

Flight tracks were established in the BOREAS SSA (130 km × 90 km), located about 90 km to the north of Prince Albert, Saskatchewan. Fig. 1 shows a typical flight pattern, leaving Prince Albert airport, flying an agricultural track en-route to the SSA, where a grid pattern was flown as well as tracks over the old black spruce tower site. Flight tracks and altitude are maintained by on-board GPS navigation equipment, while airspeed and altitude above surface elements (measured with a radar altimeter) were maintained at approximately 60 m s^{-1} and 35 m, respectively. The dominant surface coverage for these patterns in the north-east of the SSA (Barr et al., 1997; Chen et al., 1999) is

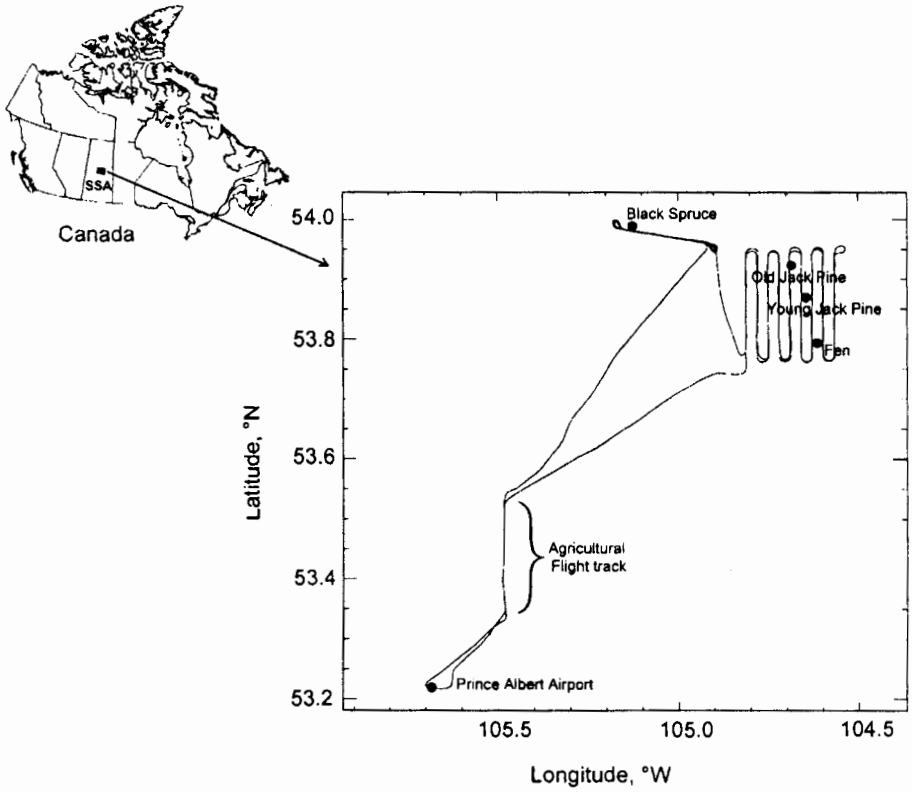

Fig. 1. Twin Otter flight tracks over forest and agriculture in BOREAS Southern Study Area. Flux tower sites are indicated (*).

60% wet conifers, typically black spruce, with a canopy height of about 10m. Regenerating areas, mostly deciduous, cover about 14% (with typical canopy heights less than 10 m); mixed forest covers 12%, fen 6%, dry conifer 4% (with some mature trees having a canopy height of 14 m), with the remainder deciduous (2%) and disturbed forest (1%). More details are given in Chen et al. (1999). This mixture of surface elements was represented by a grid pattern flight track (16 km × 16 km), consisting of nine parallel tracks, 2 km apart. On any given day, these parallel flight tracks were flown either in an east-west or north-south direction whichever was closest to crosswind. This grid pattern included passes over stands dominated by old jack pine, young jack pine, and fen vegetation. Because of the dominance of wet conifer surface elements, an additional flight track 14 km in length that consisted almost exclusively of 10 m tall mature black spruce was flown regularly. En-route to the forested areas from Prince Albert, an agricultural flight track 18.5 km in length, oriented north-south was also flown. This flight track was fairly typical of the 30 Mha that are cultivated in the Canadian prairies. It consisted of a wide variety of crops including canola, wheat, barley, flax, a few pea fields and hay and several fields under fallow.

Table 1 lists the calendar days used in the analysis, and the mean decimal times (UTC) of data collection over the agricultural area, boreal forest and the Old Black Spruce (OBS) flux tower (if this was flown on that day); together with the mean height above the vegetation of the measurements, and three parameters that will be discussed in Section 3(e) later: measured greenness and computed roughness length and Monin-Obukhov length. For the group of days as a whole the mean time of the flights is close to local noon. The agricultural runs were flown before and after the forest flights, so they may have the same mean time but they will usually be flown at a slightly larger solar zenith angle. However, the mean downward short-wave radiation and temperature are similar for both, so the different characteristics of the surfaces can be compared.

3. Comparison of agricultural and forest fluxes and state variables

3.1. Surface radiation budget

Fig. 2a shows SW_{down} and R_{net} for the daily mean of the forest runs with the daily mean of the agricultural runs. Despite some scatter (the times of the individual

Table 1
Daily parameters for flights over agricultural area, boreal forest and old Black Spruce flux tower (if flown)

Day	Year	UTC	Z (m)	Greenness Agriculture	Z_{0m} (m)	L_v (m)	UTC	Z (m)	Greenness Forest	Z_{0m} (m)	L_v (m)	UTC	Z (m)	Greenness Black spruce	Z_{0m} (m)	L_v (m)
145	1994	16.20	37	1.25	0.34	−7	17.53	31	2.18	1.64	−12					
146	1994	17.55	28	1.24	0.13	−92	17.54	30	2.11	1.74	−208					
147	1994	17.68	30	1.24	0.09	−96	18.97	32	2.16	1.33	−309	19.06	26	2.07	1.20	−279
149	1994	17.21	29	1.22	0.04	−85	17.07	60	2.23	1.42	−54					
151	1994	17.83	33	1.27	0.03	−20	18.04	24	2.24	2.15	−216					
152	1994	17.25	27	1.26	0.08	−124	18.56	60	2.33	1.52	−192	18.22	58	2.18	1.60	−166
155	1994	17.86	31	1.27	0.04	−7	17.61	41	2.17	1.83	−29	18.64	40	2.05	2.90	−14
157	1994	16.43	28	1.38	0.09	−96	17.50	34	2.85	1.80	−329					
191	1996	18.07	32	2.96	0.20	−187	18.07	39	2.32	1.87	−188					
192	1996	17.48	34	2.57	0.20	−586	17.58	42	2.04	2.05	−261	17.19	44	2.03	1.60	−254
193	1996	19.42	30	2.94	1.46	−82	18.42	39	2.17	1.96	−155	18.76	38	2.14	1.84	−129
201	1994	17.95	31	3.12	0.12	−220	17.99	39	2.71	1.53	−416					
202	1994	21.07	32	3.21	0.03	−211	22.06	35	2.83	1.29	−319	21.74	34	2.56	1.27	−257
202	1996	17.07	26	3.03	0.53	−14	16.31	36	2.22	1.25	−86					
204	1994	18.75	35	3.01	0.15	−130	17.70	39	2.79	1.99	−1090	17.75	38	2.57	1.44	−1076
205	1994	19.51	34	3.23	0.11	−97	18.84	47	2.82	1.57	−162					
206	1994	16.33	33	3.38	0.28	−15	18.01	37	2.94	1.98	−80	17.93	36	2.69	1.63	−82
207	1994	18.30	33	3.02	0.24	−30	18.31	39	2.74	2.30	−45	19.30	41	2.67	1.78	−42
208	1994	16.70	31	3.14	0.49	−23	17.31	43	3.42	1.25	−76					
208	1996	21.43	32	2.84	0.83	−14	20.28	38	2.17	1.70	−78					
209	1996	17.02	31	2.82	0.37	−176	18.33	34	2.17	1.65	−455	19.29	39	1.87	1.54	−659
211	1996	16.92	33	2.89	0.26	−14	16.99	35	2.20	1.74	−30	16.01	35	2.08	1.39	−29
251	1994	21.40	31	1.22	0.11	−5	20.44	35	2.54	1.41	−71					
254	1994	17.89	34	1.29	0.12	−30	18.05	36	2.17	1.92	−188					
255	1994	19.30	31	1.27		(0)	18.46	40	2.34	1.40	−188	17.74	37	2.15	1.93	−215
256	1994	17.92	32	1.27	0.12	−50	17.97	33	2.24	1.97	−226	18.77	39	2.18	1.25	−216
258	1994	21.95	32	1.26	0.05	−74	21.31	35	2.19	1.37	−318	21.31	35	2.19	1.37	−318
259	1994	18.14	32	1.18	0.05	−101	18.17	34	2.23	1.52	−371					
260	1994	19.75	31	1.16	0.59	−34	18.74	33	2.11	1.66	−83	18.77	32	2.08	0.91	−64
Mean		18.20	32	2.15	0.22	−99	18.23	38	2.39	1.73	−224	18.58	40	2.25	1.56	−233

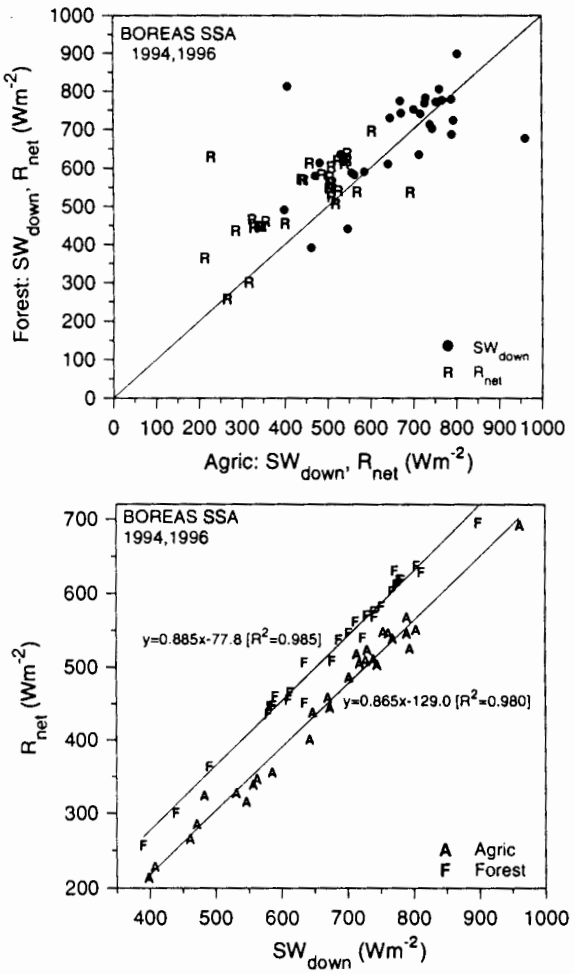

Fig. 2. Comparison of SW_{down} and R_{net} over forest and agricultural runs (upper), and (lower) dependence of R_{net} on SW_{down}, with regression fits.

flight legs are necessarily different), there is little bias between the different land surfaces in the incident solar radiation, but R_{net} is systematically higher over the forest runs. Fig. 2b plots R_{net} against SW_{down} for forest and agricultural daily means, together with the linear regression lines. For the same incident solar flux, R_{net} is 50 W m^{-2} lower over the agricultural terrain, because of the higher albedo (Fig. 5) and generally higher surface temperature (Fig. 3), which increases the outgoing longwave flux.

3.2. Air temperature, dewpoint and skin temperature

Fig. 3 plots daily means of air temperature, dewpoint and radiometric surface temperature (as symbols T, D, S) for the forest runs against the agricultural runs. There

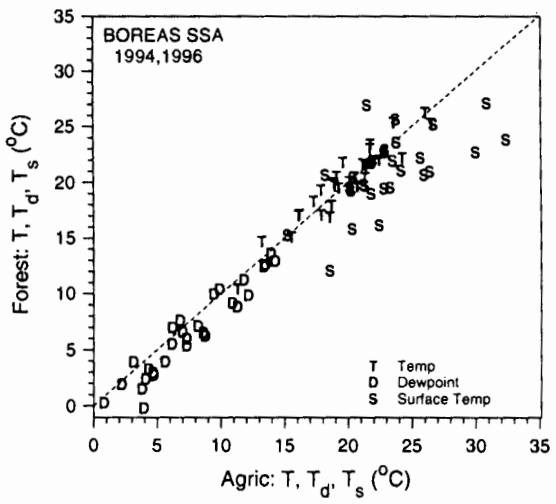

Fig. 3. Comparison of mean air temperature, dewpoint and radiometric skin temperature for forest and agricultural runs.

is little departure from the reference 1:1 line for air temperature, but dewpoint and skin temperature are generally higher for the agricultural runs. The shading of the ground and lower canopy by the canopy top is probably responsible for the lower mean radiation temperature of the forest (Sun and Mahrt, 1995). It is reasonable to conclude from Figs. 2a and 3 that the agricultural and forest runs are close enough in space and time so that differences in the surface fluxes can be attributed to differences in the land surface rather than incident radiation or atmospheric temperature.

3.3. Surface wind and stress

Fig. 4a plots daily means of wind speed, U, and friction velocity, U_{star} ($\times 10$), for the forest runs against the agricultural runs, together with the 1:1 reference line. Despite the scatter, wind speeds are similar at 35 m, but the friction velocity is systematically higher over the forest. Fig. 4b plots U_{star} against U, together with the regression line fits. For the same wind speed, U_{star} is twice as large over the forest. This is of course a consequence of the much larger roughness length (see Fig. 6a).

3.4. Comparison of forest and agriculture daily means

Fig. 5 shows different characteristics for the forest and agriculture run data. Panel (a) compares daily means of surface albedo, which is systematically higher over the agricultural land surface. Forest albedo has little seasonal variation, but over agricultural land,

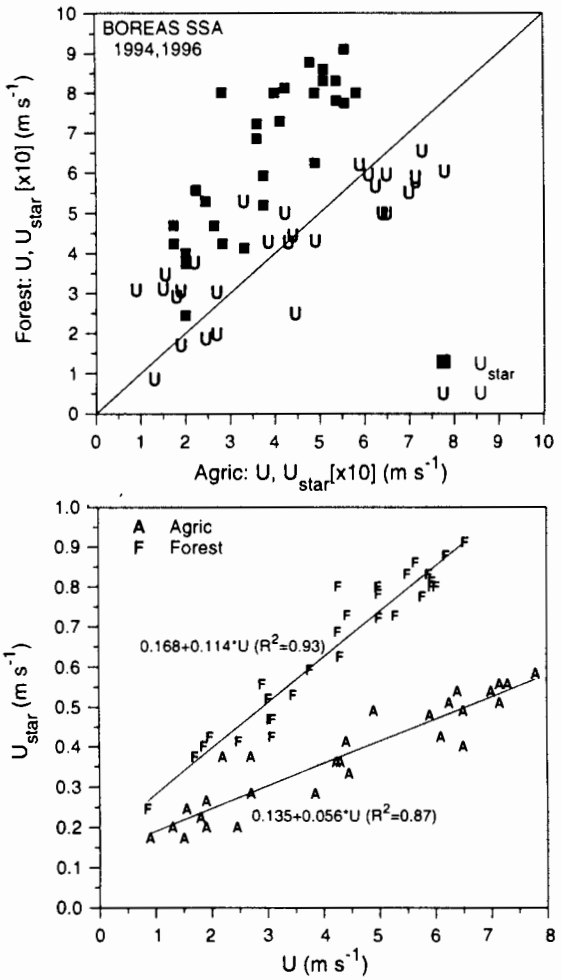

Fig. 4. Comparison of wind-speed and friction velocity (upper), and (lower) dependence of friction velocity on wind-speed, with regression fits.

albedo increases from spring to summer. Panel (b) compares the surface Bowen ratio (BR), defined as H over λE. There is considerable scatter for individual days, but Bowen ratio is systematically lower over agriculture in spring and summer, but not in the autumn. Panel (c) compares the CO_2 fluxes. Seasonal patterns are quite distinct for forest and agriculture. At the time of the aircraft flux measurements, with air temperatures well above freezing, the forest is a consistent daytime sink of CO_2, with a weak summer maximum. In contrast, the uptake of CO_2 over the agricultural land surface is much larger in summer and near zero or a weak carbon source in spring and autumn. Finally, panel (d) shows water use efficiency (WUE) defined as the ratio of the CO_2 flux/water vapor flux (mg CO_2/g H_2O). This largely reflects that the CO_2 flux has a rather small variation over forest. Over the agricultural land, WUE is small and positive when the fields are releasing carbon dioxide prior to leaf emergence and following senescence. During the growing season the forest is more efficient in its water use than the agricultural land. One extreme point corresponded to an agricultural flux run under overcast conditions.

3.5. Seasonal comparison of forest and agricultural landscapes

Table 1 shows the daily mean for each vegetation type of the radar height of the measurements above the vegetation, the measured Greenness index, the roughness length, Z_{0m}, and Monin-Obukhov length, L_v, calculated from the friction velocity and virtual heat flux. We fitted the Monin-Obukhov solutions (using the formulation used by Betts and Beljaars, 1993) at the aircraft flight level (about 35 m radar height; we assumed zero displacement height, as the radar has little penetration of the canopy) to the fluxes for each track of a pattern, and from these computed a daily mean over agricultural runs, forest and the mature black spruce tower site (which was also flown on a subset of the days). The flight days fall into three seasonal groups as shown, so we computed a seasonal mean (with a standard deviation among the days in each seasonal group) for the selected fields shown in Fig. 6. Panel (a) shows mean roughness length. Not surprisingly, the momentum roughness length over the forest was 1.7 m, an order of magnitude greater than over the agricultural terrain, consistent with the difference in friction velocity shown in Fig. 4. Table 1 shows the correspondingly larger negative values of the Monin-Obukhov length. Panel (b) shows mean albedo (left-hand-scale) and measured Greenness index (middle curves, right-hand-scale), calculated as the ratio of near-infrared (730 nm) to red (660 nm) radiation. The old black spruce site has a slightly lower albedo and lower greenness index than the mean of the forest runs, which include some mixture of deciduous trees (such as aspen) and fens, in addition to coniferous species. Greenness for the agricultural land is low in spring and fall with a sharp summer peak. Panel (c) shows the sensible and latent heat fluxes for the three composites and panel (d) the mean Bowen ratio. The black spruce site has in all seasons a higher Bowen ratio than the forest composite, and correspondingly lower latent and higher sensible heat fluxes. The sensible heat flux is much lower over agricultural land in spring and summer, when the corresponding Bowen ratio is lower than over the forest (Fig. 5b).

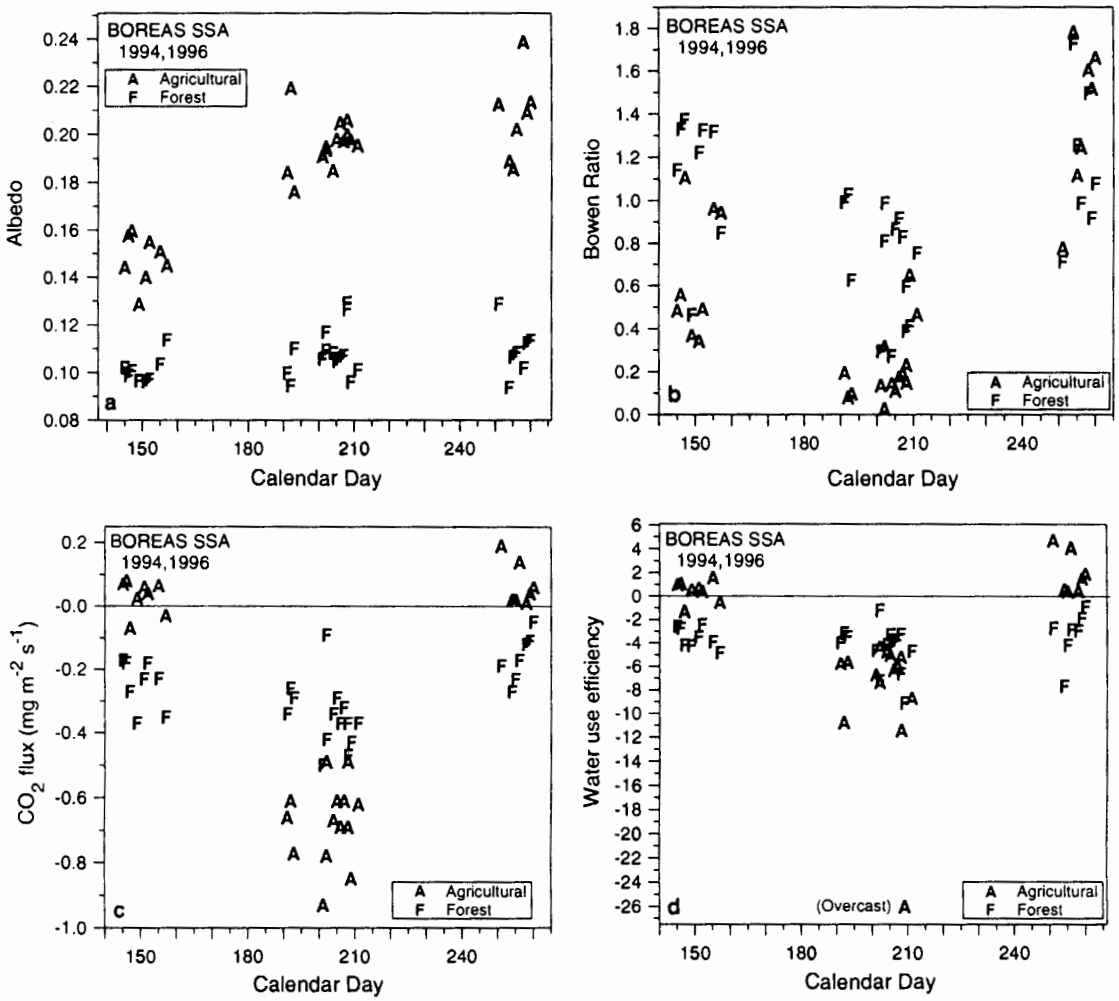

Fig. 5. Comparison of forest and agricultural daily means for: (a) albedo, (b) Bowen ratio, (c) CO_2 flux and (d) water use efficiency.

4. Daily radiation balance over grass and conifer sites

4.1. Daily mean albedo, SW_{down} and R_{net} from flux tower sites

The Twin Otter flights discussed in the previous section covered the spring, summer and autumn season comparisons between forest and agricultural landscapes, and are centered near local noon. It is useful to compare also the daily mean radiation fluxes for forest and low vegetation, both with and without snow cover. In the winter season with temperatures generally well below zero (monthly mean values around −20 °C in January and February), the primary difference between forest and unforested sites is in surface albedo. Grassland and agricultural sites are snow covered, with a high albedo, while albedo remains low for forest sites, where the snow is shaded by the trees (e.g. Pomeroy and Dion, 1996; Betts and Ball, 1997). This has a large impact on the surface R_{net}. Although we have no aircraft data comparing sites on the same day, there were 10 mesonet sites operating during BOREAS: 2 over grass and 7 over predominantly coniferous forest (Shewchuk, 1997). For the years 1994 and 1995, daily means of incident and reflected short-wave and net radiation were generated for each site. The days were then subsetted into those days with snow on the ground, and those days without snow cover. These data were then composited in 50 W m^{-2} bins of downward short-wave flux. Fig. 7a shows albedo for grass and conifer sites, calculated from daily averages (Betts and Ball, 1997). Albedo over snow covered grass is in the range 0.7 to 0.8. At the cold temperatures in Saskatchewan, snow ages rather slowly.

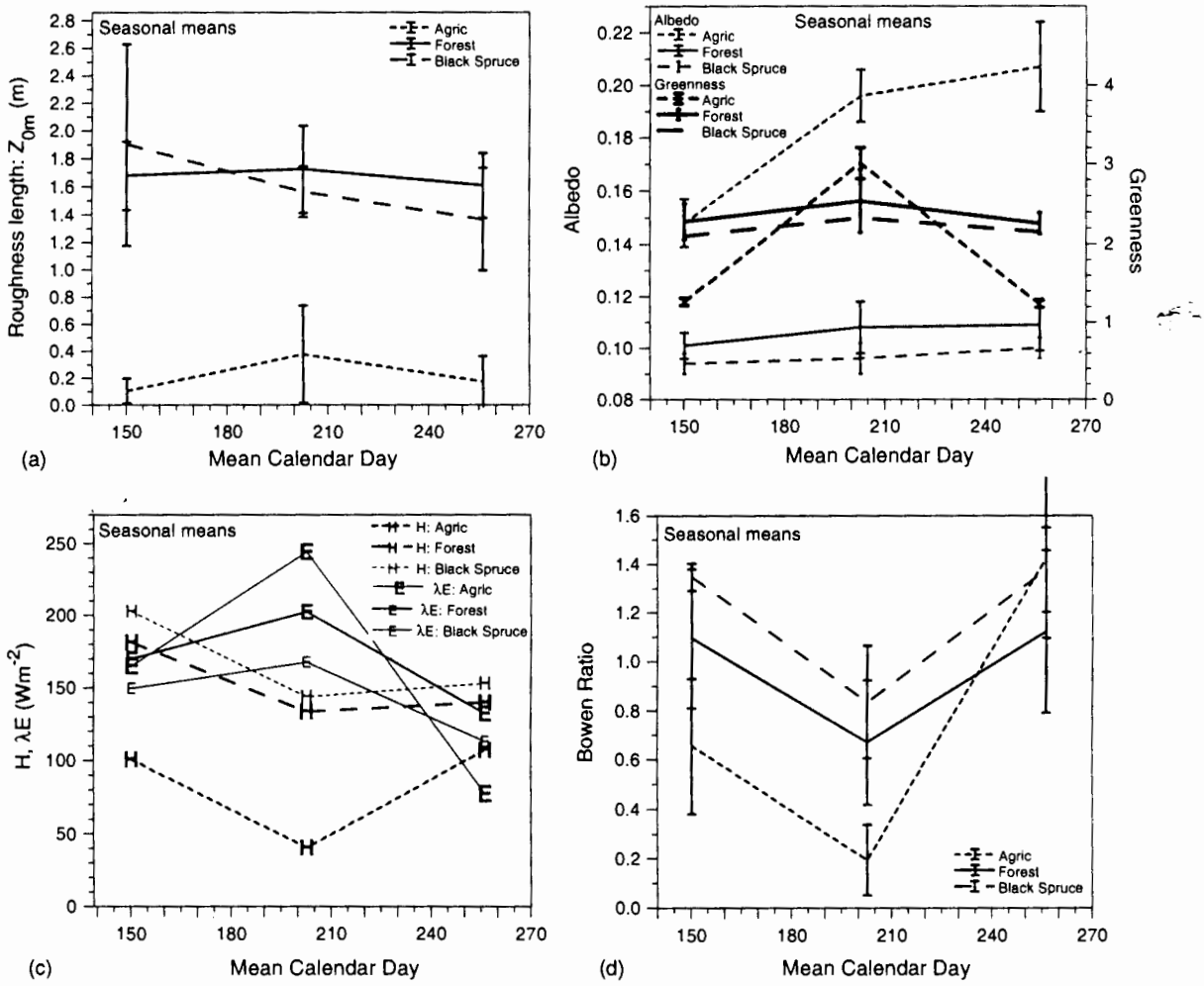

Fig. 6. Seasonal means of: (a) roughness length, (b) albedo and greenness index, (c) sensible and latent heat and (d) Bowen ratio.

For the forest sites, where the snow is beneath the canopy, albedo is low, generally below 0.2, and decreases slightly with increasing solar flux, probably because albedo increases with the fraction of diffuse radiation (Betts and Ball, 1997). The snow melts later in the spring under the canopy than over grass; which is why the lower curve extends to higher mean values of SW_{down}. We also show the corresponding curves with no snow cover, when both surfaces have lower albedos: of order 0.2 for grass and 0.1 for forest sites.

Fig. 7b plots R_{net} as a function of SW_{down} for grass and forest sites, both with and without snow. This shows the very large difference in winter in the surface energy balance for the two classes of vegetation, and the much smaller difference in summer. Snow under the forest canopy, although it is present for longer periods than over grass and agricultural sites, has only a small impact on the net radiation. The surface albedo is largely determined by the canopy, and the canopy is snow-free most of the time even in winter. Snowfall remains on the canopy only in deep winter, when solar radiation levels are very low, and provided wind conditions are calm (see Betts and Ball, 1997). In sharp contrast, R_{net} is reduced to very low values over snow covered surfaces, because of the high albedo. In summer, the difference between forest and grass in daily mean R_{net} is about 15 W m^{-2}. This is only a third of the difference between forest and agriculture shown in Fig. 2b near local noon.

4.2. R_{net} differences from regression fits

Four linear regression lines were computed through the mean data in Fig. 7b, both for comparison with Fig. 2b, and to estimate the monthly and annual

difference in R_{net} for grass and forest land surface for the same SW_{down}.

Forest : no snow $R_{net} = -12.6 + 0.66 \times SW_{down}$ $[R^2 = 0.999]$ (2a)

Grass : no snow $R_{net} = -15.2 + 0.60 \times SW_{down}$ $[R^2 = 0.997]$ (2b)

Forest : with snow $R_{net} = -22.9 + 0.65 \times SW_{down}$ $[R^2 = 0.992]$ (2c)

Grass : with snow $R_{net} = -13.2 + 0.18 \times SW_{down}$ $[R^2 = 0.885]$ (2d)

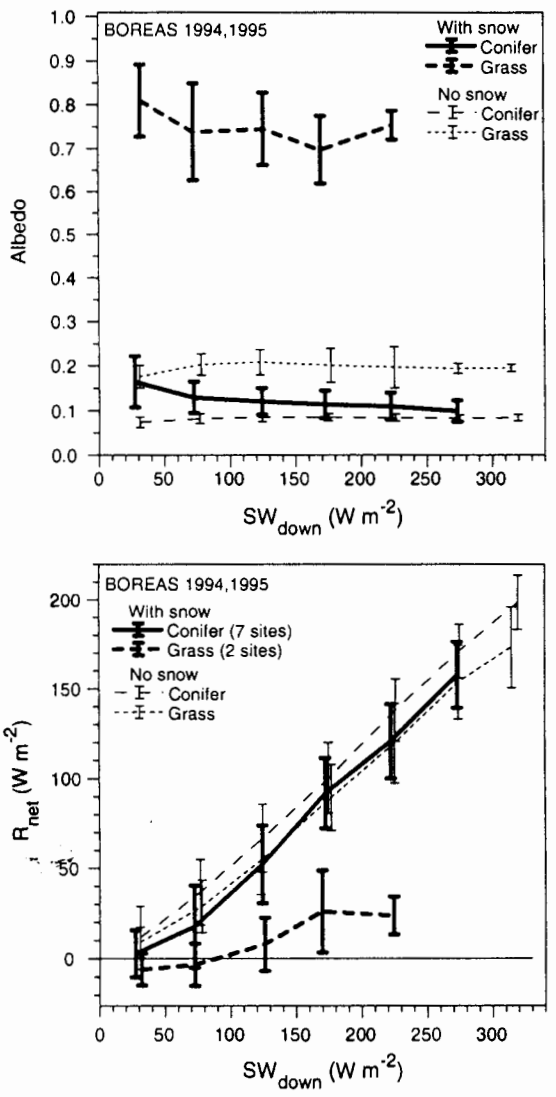

Fig. 7. Albedo and R_{net} for conifer and grass sites, with and without snow, as a function of SW_{down}.

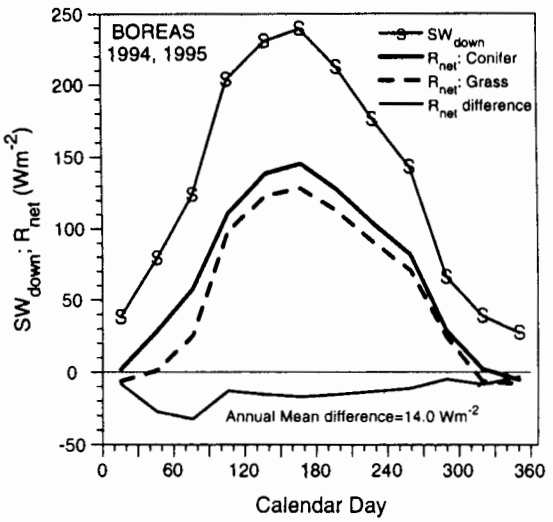

Fig. 8. Annual cycle of mean SW_{down}, R_{net} for conifer and grass sites and their difference.

Fig. 8 shows the mean annual cycle of SW_{down} averaged over all nine of these BOREAS sites. The middle curves are R_{net} for grass and forest, computed using the regression fits, together with the fraction of days each month when the ground was snow covered. In each month, R_{net} is less over grass than forest. The lowest curve shows the difference, which reaches 32 W m^{-2} in March. The mean annual difference between grass and forest land cover for the same incoming short-wave is 14 W m^{-2}.

5. Feedback between surface Bowen ratio, and cloud and radiation fields

Sections 3 and 4 show the difference between forest and agricultural or grassland sites in the same region for similar conditions of incoming short-wave flux and atmospheric temperature and humidity. The dominant surface cover is forest, which determines the mean structure of the boundary layer, and the local cloud cover. If the surface were transformed from forest to agriculture over a large area, important interactions between the surface, the boundary layer and the cloud fields that feedback on the surface energy budget must be considered (Betts, 2004; Betts and Viterbo, 2005). Observations are not available; therefore model data from the ECMWF 40-year reanalysis (ERA40) will be used to indicate the sense and probable magnitude of this feedback. The ERA40 land-surface model (Van den Hurk et al., 2000) was developed using data from BOREAS, therefore the biases of the model data from observations are relatively small (Betts et al., 2001b, 2003). We have an hourly archive from ERA40 of surface fluxes, meteorological

data and cloud fraction at [54°N, 105°W], representative of the BOREAS SSA (see Fig. 1). From this time-series, daily means were calculated, and composites from these daily data for the warm season (May, June, July and August) from the 10 years, 1993–2002 are presented. Fig. 9 (top) shows the surface energy budget (net shortwave, SW_{net}, net longwave, LW_{net}, R_{net}, λE, H and ground heat flux, G) as a function of daily mean SW_{down}. The model fluxes are almost linear functions of SW_{down}, although λE increases rather weakly. Since the daily variation of SW_{down} in these months on clear days is small, most of the variation of SW_{down} is caused by variations in mean cloud cover. The lower plot is similar, but as a function of daily mean lifting condensation level in pressure co-ordinates (P_{LCL}), which we may consider to be representative of a mean cloud-base. The fluxes are more non-linear, and their range is generally reduced, but both SW_{down} and LW_{down} get larger as the mean sub-cloud layer deepens. This suggests that the mean cloud cover decreases as mean cloud-base P_{LCL} increases.

The coupling of the fluxes with SW_{down} is of interest for comparison with the earlier observational results. We computed linear regression lines through the mean data in Fig. 9a for the six fluxes.

$$SW_{net} = -0.1 + 0.877 \times SW_{down}, \quad [R^2 = 1] \tag{3a}$$

$$R_{net} = -3 + 0.609 \times SW_{down}, \quad [R^2 = 0.999] \tag{3b}$$

$$LW_{net} = -3 - 0.3 \times SW_{down}, \quad [R^2 = 0.995] \tag{3c}$$

$$H_{net} = -38.6 + 0.389 \times SW_{down}, \quad [R^2 = 0.999] \tag{3d}$$

$$\lambda E = 38.4 + 0.13 \times SW_{down}, \quad [R^2 = 0.968] \tag{3e}$$

$$G_{net} = -2.9 + 0.093 \times SW_{down}, \quad [R^2 = 0.985] \tag{3f}$$

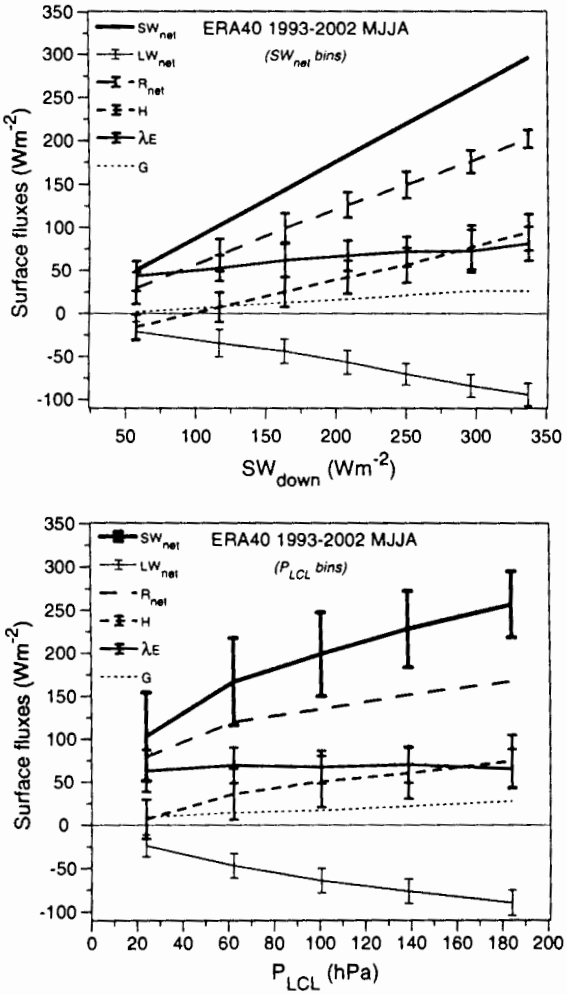

Fig. 9. Dependence of surface fluxes on SW_{down} (upper) and cloud-base P_{LCL} (lower).

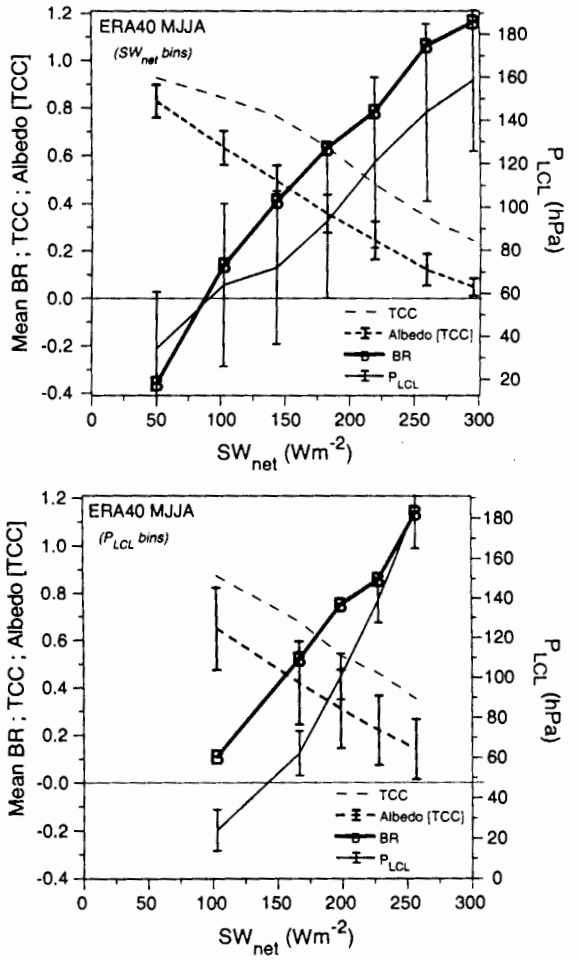

Fig. 10. Dependence of Bowen ratio, cloud cover and mean cloud-base on SW_{net}.

The slope of SW_{net} is simply one minus the model surface albedo at this gridpoint of 0.123 (in the absence of snow). The R_{net} relationship is close to that derived from the tower data (2b), differing from it by less than ± 8 W m^{-2} at the extremes of the range.

Fig. 10 shows the relationship between SW_{net} and several important variables in the ERA40 model. On the left-hand y-axis is mean BR ($=H/\lambda E$), total cloud cover, TCC, as a fraction (a model archive parameter), and a "cloud albedo". This is the albedo for the total cloud field, as seen from the surface, defined as the fraction of SW_{down}, which is reflected (or absorbed) by the cloud field

$$\text{albedo[TCC]} = 1 - \frac{SW_{down}}{SW_{down}(\max)} \quad (4)$$

where SW_{down}(max) was estimated by fitting a seasonal curve to the upper envelope of the daily data, so that it represents the upper limit of SW_{down} reaching the surface in the absence of cloud cover (that is the clear-sky SW_{down} flux). Both TCC and albedo[TCC] naturally decrease with increasing SW_{net}, while BR increases with increasing SW_{net}. On the right-hand-scale we show mean cloud-base, a measure of the depth of the mixed layer, which increases as SW_{net} and BR increase. The upper panel is from the data binned by SW_{net} (and so it has a small standard deviation for albedo[TCC], and the lower panel (kept at the same scale despite the reduced variable range) is from the data binned by the mean cloud-base P_{LCL} (consequently it has a small standard deviation in P_{LCL}). The two panels show a similar interrelation of the variables: increased cloud cover reduces surface SW_{net} and is associated with reduced BR and a lower mean cloud-base. The range of the variation of albedo[TCC] in Fig. 10 from 0.1 to 0.8 makes clear that the coupling of the cloud field to the surface evaporation and BL structure plays as important a role in the surface energy balance as the differences in albedo between surfaces (Fig. 6), even in the presence of snow (compare Fig. 7a). This is the cloud short-wave forcing at the surface. We do not know if it is correct in ERA40, since it is a function of many parameterizations, as well as the predicted cloud field, but the model data give an indication of its likely importance.

Fig. 11 remaps the same interrelationships in terms of mean surface BR, recomputed from the mean fluxes of the binned data. On the left-hand-scale is the albedo of the cloud field, and on the right, SW_{net} and R_{net}. Whether the data is binned by SW_{net} or P_{LCL}, the pattern is very similar (we have dropped error bars for clarity). In the lower panel, the drop in BR from 0.85 to 0.4

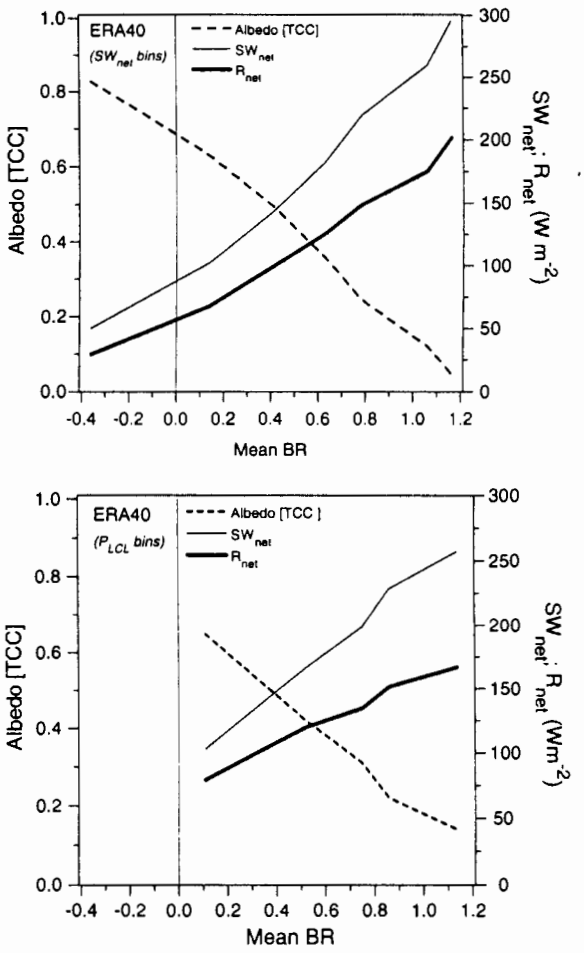

Fig. 11. Dependence of cloud albedo, SW_{net} and R_{net} on mean Bowen ratio.

corresponds in this fully interactive global model to a drop in albedo[TCC] and R_{net} of 0.21 and 32 W m^{-2}, respectively. Is this the impact we should expect from a similar difference in BR in summer between forest and agriculture (Fig. 6d)? Probably not, because the low BRs in ERA40 are associated only with days with significant precipitation, and cloud cover associated with precipitation. (In addition the albedo and roughness of the underlying surface in the model remains unchanged across this range of BR.) It is likely however, that reducing the surface BR (by replacing forest by cropland) will increase summer cloud cover, although not as much as in Fig. 11. A more plausible estimate of this increase in cloud cover with reduced BR is shown in Fig. 12, where we have extrapolated the slope of the curves above BR = 0.85 (where there is no rain; see Fig. 13, later) back to BR = 0.4. As BR drops from 0.85 to 0.4, this gives a smaller estimated change in albedo[TCC] and R_{net} of 0.13 and -25 W m^{-2},

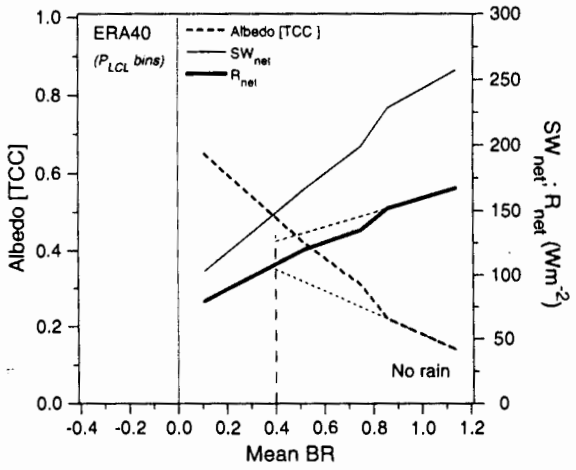

Fig. 12. Extrapolation of the impact of BR on cloud albedo and R_{net}.

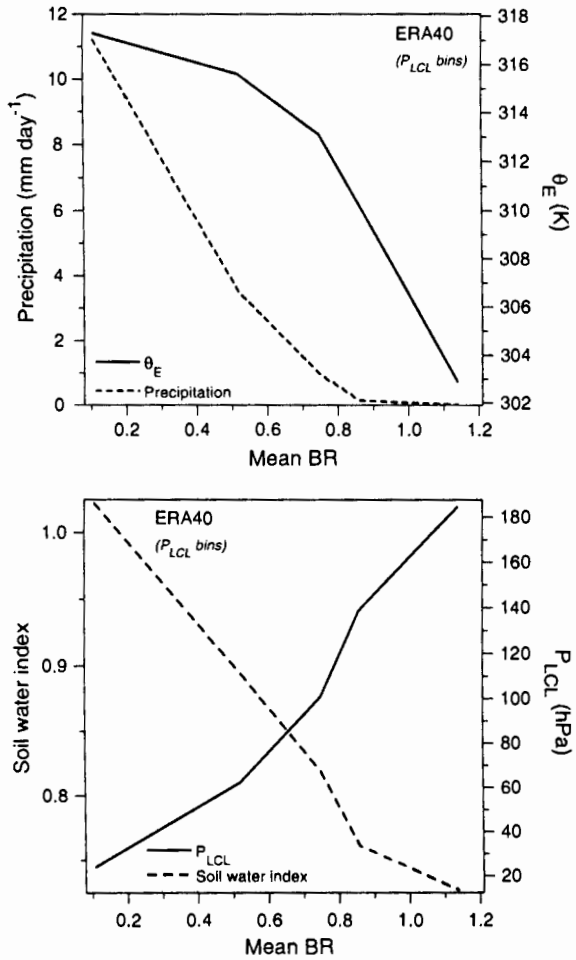

Fig. 13. Coupling between mean BR, θ_E, precipitation, soil water index and P_{LCL}.

respectively. Clearly this is only a rough estimate, but comparison with Fig. 8, shows that the increase of cloud cover with increased evaporation may be a significant perturbation on the summer and annual surface energy budget. A much more extensive analysis is needed. This simple point estimate from reanalysis data does not include the regional and global feedbacks that would result from a major shift from forest to agricultural use at this latitude. Nonetheless our results are consistent with Betts (2001) who showed that increased evaporation and cloud cover reduced SW_{down} over many mid-latitude snow-free agricultural areas, giving lower mean temperatures than in a corresponding simulation with natural vegetation.

Fig. 13 shows the coupling between mean BR, equivalent potential temperature, θ_E, precipitation, a soil water index for the upper 7 cm model soil layer, SWI, and P_{LCL}. SWI is scaled to range from 0 to 1 for soil moistures between the permanent wilting point (0.171) and field capacity (0.323) of the model soil. As BR decreases from values around 1.1, θ_E increases steeply at first while there is no precipitation, then more slowly as precipitation increases steeply at low BR. Over the same range, mean cloud-base P_{LCL} drops and the SWI increases. These relationships are physically reasonable: high summer precipitation is associated with high θ_E. At lower BR, all the processes are coupled. For example, P_{LCL} is low both because surface evaporation is high, coming from high SWI, and because the evaporation of falling precipitation brings the sub-cloud layer closer to saturation; and the precipitation of course increases SWI. Will agricultural land-use with a lower BR produce higher θ_E and more precipitation? Probably, but the exact relationships will not be the same as we see in Fig. 13, because, if large enough areas are involved, the mean rainfall will be also partly constrained by the mean evaporation (Betts, 2004).

6. Conclusions

Field data from aircraft and mesonet towers over forest, agricultural and grass sites were used to show the effect of land cover on the surface energy budget at the latitude of the boreal forest. The forest has an order of magnitude larger roughness length, and a lower albedo than the agricultural areas. Higher surface temperatures and the higher albedo over agricultural land reduce R_{net} near local noon in the warm season by about 50 W m^{-2} in comparison with the adjacent boreal forest. The forest between late May and mid-September has the smallest seasonal cycle in surface fluxes with a weak minimum of BR and a weak maximum of CO_2 uptake in mid-summer. In contrast the agricultural areas have much lower BR and

much higher uptake of CO_2 in mid-summer, but a net CO_2 release and much reduced evaporation in spring and fall. We partition 2 years of radiation data from towers over the forest and two grass sites into days with and without snow to show the dependence of daily R_{net} and albedo on incoming SW_{down} over the forest and short vegetation (here grass) in both winter, and in the warm season without snow. The mean difference in R_{net} and albedo is largest in winter. The annual average is a 14 W m^{-2} reduction in R_{net} over grass sites.

An hourly time-series from ERA40 for the BOREAS southern study area was used to explore the coupling for this site on daily timescales between the surface energy partition, the mean BL depth, the cloud field and the long-wave and short-wave radiation fields, which are all prognostic variables in this reanalysis model. In composites derived from daily means, the cloud field and the cloud surface radiative forcing are quite closely coupled to the surface BR and mean cloud-base depth. All fluxes are linear functions of the surface SW_{down}. An albedo for the total cloud cover, the cloud short-wave forcing at the surface was defined; and it shows the range 0.1–0.8 with decreasing surface BR, and plays a major role in the surface energy balance. For the reanalysis data the low values of BR correspond to days with precipitation. However, by extrapolating the dependence of albedo and R_{net} on Bowen ratio from days without rain, we make a rough estimate that this cloud feedback may increase albedo by 0.13 and reduce R_{net} by 25 W m^{-2} in summer over agricultural land with a much lower BR than the boreal forest. Clearly, more comprehensive global modeling studies are needed, since we do not address regional feedbacks on the circulation and water cycle, which might result from a lower summer BR, and larger total albedo. In the ECMWF model, increased summer evaporation gives increased precipitation (Betts, 2004), but global models differ widely in their land-surface coupling (Koster et al., 2004; Lawrence and Slingo, 2005).

Acknowledgments

Alan Betts acknowledges support from NSF under Grant ATM-0529797, and from the NASA under Grant NAS5-11578 and NEWS Grant NNG05GQ88A.

References

Barr, A.G., Betts, A.K., Desjardins, R.L., MacPherson, J.I., 1997. Comparison of regional surface fluxes from boundary-layer budgets and aircraft measurements above boreal forest. J. Geophys. Res. 102, 29213–29218.

Betts, R.A., 2000. Offset of the potential carbon sink from boreal forestation by decreases in surface albedo. Nature 408, 187–190.

Betts, R.A., 2001. Biogeophysical impacts of land use on present-day climate near-surface temperature change and radiative forcing. Atmos. Sci. Lett. 2, 39–51.

Betts, A.K., 2004. Understanding Hydrometeorology using global models. Bull. Am. Meteorol. Soc. 85, 1673–1688.

Betts, A.K., Ball, J.H., 1997. Albedo over the boreal forest. J. Geophys. Res. 102, 28901–28910.

Betts, A.K., Beljaars, A., 1993. Estimation of effective roughness length for heat and momentum from FIFE data. Atmos. Res. 30, 251–261.

Betts, A.K., Viterbo, P., 2005. Land-surface, boundary layer and cloud-field coupling over the south-western Amazon in ERA-40. J. Geophys. Res. 110, D14108, doi:10.1029/2004JD005702.

Betts, A.K., Ball, J.H., McCaughey, J.H., 2001a. Near-surface climate in the boreal forest. J. Geophys. Res. 106, 33529–33542.

Betts, A.K., Viterbo, P., Beljaars, A.C.M., van den Hurk, B.J.J.M., 2001b. Impact of BOREAS on the ECMWF Forecast Model. J. Geophys. Res. 106, 33593–33604.

Betts, A.K., Ball, J.H., Viterbo, P., 2003. Evaluation of the ERA-40 surface water budget and surface temperature for the Mackenzie River basin. J. Hydrometeorol. 4, 1194–1211.

Brovkin, V., Lewis, S., Loutre, M.-F., Crucifix, M., Claussen, M., Ganopolski, A., Kubatski, C., Petukhov, V., 2003. Stability analysis of the climate-vegetation system in high northern latitudes. Climat. Change 57, 119–138.

Charney, J.G., Quirk, W.K., Chou, S.-H., Kornfield, J., 1977. A comparative study of the effects of albedo change on drought in semi-arid regions. J. Atmos. Sci. 34, 1366–1385.

Chen, J.M., Leblanc, S.G., Cihlar, J., Desjardins, R.L., MacPherson, J.I., 1999. Extending aircraft- and tower-based CO_2 flux measurements to a boreal region using a Landsat thematic mapper land cover map. J. Geophys. Res. 104 (D14), 16859–16877.

Desjardins, R.L., MacPherson, J.I., 1991. Water vapor flux measurements from aircraft. In: Schmugge, T.J., André, J.C. (Eds.), Land Surface Evaporation: Measurement and Parameterization. Springer-Verlag, New York.

Desjardins, R.L., MacPherson, J.I., Mahrt, L., Schuepp, P., Pattey, E., Neumann, H., Baldocchi, D., Wofsy, S., Fitzfarrald, D., McCaughey, H., Joiner, D.W., 1997. Scaling up flux measurements for the boreal forest using aircraft-tower combinations. J. Geophys. Res. 102 (D24), 29125–29133.

Desjardins, R.L., MacPherson, J.I., Schuepp, P.H., 2000. Aircraft-based flux sampling strategies. In: Meyers, R.A. (Ed.), Encyclopedia of Analytical Chemistry. John Wiley and Sons Ltd., Chichester, pp. 3573–3588.

Kitoh, A., Yamasaki, K., Tokioka, T., 1988. Influence of soil moisture and surface albedo changes over the African tropical rain forest on summer climate investigated with the MRI-GCM-1. J. Meteorol. Soc. Jpn. 66, 65–85.

Koster, R.D., Dirmeyer, P.A., Guo, Z., Bonan, G., Chan, E., Cox, P., Gordon, C.T., Kanae, S., Kowalczyk, E., Lawrence, D., Liu, P., Lu, C.-H., Malyshev, S., McAvaney, B., Mitchell, K., Mocko, D., Oki, T., Oleson, K., Pitman, A., Sud, Y.C., Taylor, C.M., Verseghy, D., Vasic, R., Xue, Y., Yamada, T., 2004. Regions of strong coupling between soil moisture and precipitation. Science 305, 1138–1140.

Lawrence, D.M., Slingo, J.M., 2005. Weak land-atmosphere coupling strength in HadAM3: the role of soil moisture variability. J. Hydrometeorol. 6, 670–680.

Levis, S., Foley, J.A., Brotvin, V., Pollard, D., 1999. On the stability of the high-latitude climate-vegetation system in a coupled atmosphere-biosphere system. Global Ecol. Biogeog. 8, 489–500.

MacPherson, J.I., 1996. NRC Twin Otter Operations in BOREAS 1996. Flight Research Laboratory report LTR-FR-129. Institute for Aerospace Research, NRC, Canada.

MacPherson, J.I., Bastian, M., 1997. NRC Twin Otter Operations in BOREAS 1994. Flight Research Laboratory report LTR-FR-134. Institute for Aerospace Research, NRC, Canada.

Pomeroy, K.W., Dion, K., 1996. Winter radiation extinction and reflection in a boreal pine canopy: measurements and modeling. Hydrol. Process. 10, 1591–1608.

Price, A.G., Dunham, K., Carleton, T., Band, L., 1997. Variability of water fluxes through the black spruce (*Picea mariana*) canopy and feather moss (*Pleurozium schreberi*) carpet in the boreal forest of northern Manitoba. J. Hydrol. 196, 310–323.

Sellers, P.J., Hall, F.G., Kelly, R.D., Black, A., Baldocchi, D., Berry, J., Ryan, M., Ranson, K.J., Crill, P.M., Lettenmaier, D.P., Margolis, H., Cihlar, J., Newcomer, J., Fitzjarrald, D., Jarvis, P.G., Gower, S.T., Halliwell, D., Williams, D., Goodison, B., Wickland, D.E., Guertin, F.E., 1997. BOREAS in 1997. Experiment overview, scientific results, and future directions. J. Geophys. Res. 102 28 731-28 769.

Shewchuk, S.R., 1997. The surface atmospheric sciences mesonet for BOREAS. J. Geophys. Res. 102, 29077–29082.

Sud, Y.C., Shukla, J., Mintz, Y., 1988. Influence of land-surface roughness on atmospheric circulation and rainfall: a sensitivity study with a general circulation model. J. Appl. Meteorol. 27, 1036–1054.

Sun, J., Mahrt, L., 1995. Relationship of the heat flux to microscale temperature variations: application to BOREAS. Boundary Layer Meteorol. 76, 291–301.

Van den Hurk, B.J.J.M., Viterbo, P., Beljaars, A.C.M., Betts, A.K., 2000. Offline validation of the ERA40 surface scheme. ECMWF Tech Memo. 295, 43 pp., available at http://www.ecmwf.int/publications/library/ecpublications/_pdf/tm/001-300/tm295.pdf.

Walker, J., Rowntree, J.R., 1977. The effect of soil moisture on circulation and rainfall in a tropical model. Quart. J. Roy. Meteorol. Soc. 103, 29–46.

Xue, Y., 1997. Biosphere feedback on regional climate in tropical north Africa. Quart. J. Roy. Meteorol. Soc. 123, 1483–1515.

Xue, Y., Shukla, J., 1993. The influence of land-surface properties on Sahel climate. Part I. Desertification. J. Climate 6, 2232–2245.

Zhu, T., Wang, D., Desjardins, R.L., MacPherson, J.I., 1999. Aircraft-based volatile organic compounds flux measurements with relaxed eddy accumulation. Atmos. Environ. 33, 1969–1979.